Microporous and Mesoporous Materials 263 (2018) 28–33

Contents lists available at ScienceDirect

Microporous and Mesoporous Materials

journal homepage: www.elsevier.com/locate/micromeso

# Nanostructured silver silica materials as potential propolis carriers

Margarita Popova[a,*], Hristina Lazarova[a], Boryana Trusheva[a], Milena Popova[a], Vassya Bankova[a], Judith Mihály[b], Hristo Najdenski[c], Iva Tsvetkova[c], Ágnes Szegedi[b]

[a] Institute of Organic Chemistry with Centre of Phytochemistry, Bulgarian Academy of Sciences, 1113 Sofia, Bulgaria
[b] Research Centre for Natural Sciences, Institute of Materials and Environmental Chemistry, Hungarian Academy of Sciences, 1117 Budapest, Hungary
[c] The Stefan Angeloff Institute of Microbiology, Bulgarian Academy of Sciences, 1113 Sofia, Bulgaria

ARTICLE INFO

*Keywords:*
Silver nanoporous silica
MCM-41
SBA-15
Poplar propolis
Antimicrobial effect

ABSTRACT

It is reported for first time, that silver modified nanoporous MCM-41 or SBA-15 silicas are promising carriers for the preparation of poplar propolis loaded dermal formulations. MCM-41 or SBA-15 were successfully modified with 5–15 nm sized silver nanoparticles by direct or post synthesis methods. The formed silver nanoparticles are stabilized in the channels or on the outer surface of nanoporous supports. Poplar propolis molecules were loaded into the mesoporous channels by impregnation. The parent and poplar propolis loaded formulations were characterized by powder XRD, $N_2$ physisorption, thermal analysis and ATR FT-IR spectroscopy. *In vitro* release of poplar propolis and silver was studied in phosphate buffer at pH = 5.5 which is typical for dermal formulations. Adsorption of poplar propolis on nanoporous silica particles significantly improves its water solubility. Moreover propolis loaded silver-silica systems show significantly better antibacterial and antifungal activities than poplar propolis and silver-modified carriers themselves.

## 1. Introduction

In the recent years many mesoporous silica based drug delivery systems have been developed [1,2]. Mesoporous SBA-15 or MCM-41 silica carriers are biocompatible materials and both of them have the capability to load e.g. nanosized metal particles into the channels or to be functionalized with organic groups [2,3]. Thus the effect of controlled drug release can be combined with the antibacterial effect of metallic nanoparticles, such as silver. Silver nanoparticles can be stabilized in the channels or on the outer surface of mesoporous silica supports, and besides the empty channels can be loaded by bioactive molecules. Silver nanoparticle containing nanoporous silica materials can be easily synthesized by direct synthesis or by post-synthesis modification (template ion-exchange) methods [4,5]. In our previous study [6], it was shown that silver modified MCM-41 and SBA-15 materials are suitable carriers for drugs such as sulfadiazine to design a drug-delivery system with improved bioavailability and antibacterial activity for the treatment of burn wound infections.

Propolis is a resinous hive product containing beeswax and plant exudates collected by honeybees from certain plant sources. It has well known pharmacological properties as an anti-inflammatory, anticancer, antioxidant, antibacterial, antiviral and antifungal agent [7–10]. It is used in traditional medicine in the form of alcohol extracts or in combination with other natural products. The composition of propolis is very complex and varies depending on the phytogeographic diversity of the collection area and the season [11–15]. As a result of the variability of plant sources, in distinct geographic regions the antibacterial compounds in bee glue are different, for example, flavonoids and cinnamic acid derivatives in European samples, diterpenic acids and prenylated coumaric acids in Brazilian, etc. [12,15,16]. The main problem restricting propolis diverse application is its very low water solubility. Therefore, there is a pressing need to find a novel approach that can harness the potential of propolis in the clinical practice. Some recent preliminary studies reported the encapsulation of propolis extract in nanoparticulate systems [17–19]. Moreover, honey and propolis are very efficient for treatment of infected wounds thus some authors have reported the preparation of lipid system loaded with propolis for wound healing [20–22].

**In this study** silver nanoparticle containing mesoporous silica Ag-SBA-15 and Ag-MCM-41 carriers were loaded with poplar propolis in order to prepare a drug delivery system overcoming the disadvantages of propolis related to its poor solubility. To the best of our knowledge this is the first attempt to prepare propolis loaded nanoporous silica materials, possessing high antimicrobial activity.

* Corresponding author.
*E-mail address:* mpopova@orgchm.bas.bg (M. Popova).

https://doi.org/10.1016/j.micromeso.2017.11.043
Received 21 August 2017; Received in revised form 22 November 2017; Accepted 27 November 2017
Available online 02 December 2017
1387-1811/ © 2017 Elsevier Inc. All rights reserved.

## 2. Experimental section

### 2.1. Propolis sample

The raw poplar propolis used in this study was collected in the region of the town of Elena, Bulgaria. Propolis was cooled in a refrigerator, ground and extracted twice with 70% ethanol (1:10, w:v) at room temperature for 24 h. The mixture of two extracts was evaporated to dryness and the resulted propolis extract was used for loading on silver modified nanoporous materials. For determination of the studied propolis content (Table 1), a small part of this extract was subjected to GC-MS analysis after silylation (5 mg of the residue was mixed with 50 μL of dry pyridine and 75 μL of BSTFA (bis-(trimethylsilyl)-trifluoroacteamide) and heated at 80 °C for 20 min) [14]. The GC-MS analysis was performed with a Hewlett–Packard gas chromatograph 5890 series II Plus linked to a Hewlett–Packard 5972 mass spectrometer system equipped with a 30 m long, 0.25 mm i.d., and 0.15 μm film thickness DB-17HT capillary column. The temperature was programmed from 80 to 320 °C at a rate of 5 °C/min, and a 10 min hold at 320 °C. Helium was used as a carrier gas at a flow rate of 0.8 mL/min. The split ratio was 1:25, the injector temperature 280 °C, the interface temperature 300 °C, and the ionisation voltage 70 eV. Semiquantification was carried out by internal normalisation with the area of each compound. The addition of individual areas of the compounds corresponds to 100% area.

### 2.2. Synthesis of Si-MCM-41 and Ag-MCM-41 material

Spherical nanosized (100 nm) MCM-41 particles were prepared according to the procedure of Huh et al. [23]. This sol-gel procedure is carried out at 80 °C in water solution with NaOH as a catalyst. The silica source was tetraethyl orthosilicate (TEOS), and hexadecyltrimethylammonium bromide ($C_{16}$TMABr) was applied as template. The molar composition of the reaction mixture was: 1 TEOS: 0.12 $C_{16}$TMABr: 0.31 NaOH: 1190 $H_2O$. The obtained gel was aged at 80 °C for 2 h. The resulted solid was washed with distilled water until neutral pH, and dried at room temperature. Template ion-exchange method (TIE) [24,25] was used for loading of silver nanoparticles on the silica carrier and the final silver content of 5.5 wt.% was achieved with Si/Ag = 5 ratio. MCM-41 material was ion-exchanged by refluxing it at 80 °C with 0.036 M $AgNO_3$ solution (50 mL/g silica) for 20 h, and then filtered, and washed with distilled water until chloride free. The template was removed in air at 550 °C for 5 h with a heating rate of 1 °C/min. Silver containing MCM-41 sample prepared by template ion-exchange method was designated as Ag-MCM-41.

### 2.3. Synthesis of Ag-SBA-15 support

Direct hydrothermal synthesis of mesoporous Ag-SBA-15 material was carried out by modified procedure of Zhu et al. [26] in the presence of triblock copolymer P123 (BASF) as a template and TEOS as a silica source. The synthesis mixture contains 4 g of P123, 120 g of deionized water and 18.8 g of 65 wt.% nitric acid. The starting ingredients were mixed and stirred for 1 h at 40 °C. Silver nitrate was used as silver source and 0.34 g of it was added to the solution and stirred for 1 h at 40 °C. At the end 8.4 g of TEOS was added to the synthesis gel and was stirred for 20 h at 40 °C. The final molar ratio of the synthesis gel was: 1 TEOS: 0.017 P123: 0.05 $AgNO_3$: 4.93 $HNO_3$: 177.9 $H_2O$. The final suspension was aged at 100 °C for 48 h in a Teflon lined stainless steel autoclave without stirring. The obtained material was filtered, washed with distillated water until nitrate free and calcined in air at 450 °C of 1 °C/min rate for 5 h. Directly synthesized Ag-containing SBA-15 sample was designated as Ag-SBA-15.

**Table 1**
Chemical composition of ethanol extract of propolis sample (% of total ion current).[a]

| Compound | % of TIC |
|---|---|
| **Aromatic acid** | **6.6** |
| Benzoic acid | 0.6 |
| Cinnamic acid | 0.1 |
| *p*-Hydroxybenzoic acid | 0.1 |
| *p*-Methoxycinnamic acid | 0.2 |
| p-Coumaric acid | 0.6 |
| Dimethoxycinnamic acid | 1.1 |
| Ferulic acid (Z) | 0.8 |
| Ferulic acid (E) | 0.8 |
| Caffeic acid | 0.2 |
| Caffeic acid | 2.1 |
| **Phenolic acid esters** | **13.0** |
| Pentenyl coumarate | 0.1 |
| Pentenyl coumarate (isomer) | 0.2 |
| 3-Methyl-3-butenyl ferulate | 0.1 |
| 3-Methyl-3-butenyl caffeate | 1.5 |
| 2-Methyl-2-butenyl ferulate | 0.1 |
| 3-Methyl-2-butenyl ferulate | 0.9 |
| 2-Methyl-2-butenyl caffeate | 0.6 |
| 3-Methyl-2-butenyl caffeate | 1.9 |
| Phenylethyl p-coumarate | 0.1 |
| Benzyl caffeate | 2.3 |
| Benzyl ferulate | 0.2 |
| Cinnamyl caffeate | 1.3 |
| Phenylethyl caffeate | 3.7 |
| **Chalcones** | **1.6** |
| Pinocembrin chalcone | 1.0 |
| Trihydroxymonomethoxy chalcone m/z = 502 | 0.2 |
| Pinobanksinacetate chalcone | 0.4 |
| **Flavanones and dihydroflavonols** | **37.3** |
| Pinobanksin | 5.2 |
| Pinocembrin | 10.4 |
| Sakuranetin | 0.2 |
| Dihydroxymethoxyflavanone | 2.1 |
| 3-Acetylpinobanksin | 14.4 |
| Pinobanksin butanoate | 0.7 |
| Pinobanksin propanoate | 1.6 |
| Pinobanksin pentanoate | 1.8 |
| Alpinone | 0.2 |
| Pinobanksin pentenoate | 0.7 |
| **Flavones and flavonols** | **22.6** |
| Galangin | 8.2 |
| Chrysin | 7.6 |
| Dihydroxymonomethoxy flavone | 0.8 |
| Kaempferol | 0.9 |
| Quercetin | 1.1 |
| Kaempferol methyl ether | 1.3 |
| Quercetin-methyl ether | 1.2 |
| Quercetin-methyl ether (isomere) | 0.7 |
| Quercetin-methyl ether (isomere) | 0.6 |

[a] Total ion current.

### 2.4. Loading of poplar propolis on silver modified nanoporous materials

Propolis loading was carried out from ethanol solution (70%) at 37 °C applying 250 mg of propolis extract per 250 mg support. After incubation for 24 h, the mixtures were centrifuged at 15,000 rpm, rinsed with distilled water, separated by a second centrifugation, and finely dried at room temperature under vacuum. Propolis loaded Ag-MCM-41 and Ag-SBA-15 samples were designated as Ag-MCM-41/Pr and Ag-SBA-15/Pr, respectively.

The encapsulation efficiency was calculated by measuring the amount of free propolis present in the different formulations [27]. The amount of propolis in each fraction was determined by UV Vis method (292 nm, Jasco V-670). The amount of encapsulated propolis was calculated with the formula given below:

Encapsulation efficiency (%) = ((total amount of propolis - free propolis)/(total amount of propolis))*100.

### 2.5. Characterization

X-ray powder diffraction patterns were recorded by a Philips PW 1810/3710 diffractometer with Bregg-Brentano parafocusing geometry applying monochromatized CuKα (λ = 0.15418 nm) radiation (40 kV, 35 mA) and a proportional counter. Metallic silver was identified based on ICDD database PDF2, using entry 04–0783 for Ag4f. Crystallite size of metallic silver was determined by the Sherrer equation evaluating the FWMH values with full profile fitting method.

Nitrogen physisorption measurements were carried out at −197 °C using Thermo Science Surfer apparatus. The specific surface area was calculated by the BET method in the range of relative pressures from 0.01 to 0.2. The pore-size distribution was calculated from desorption branch of the isotherms with the BJH method. Silica samples were pretreated at 250 °C, whereas drug loaded materials at 80 °C for 5 h before measurements.

Silver content of the prepared samples was determined by Atomic Absorption Spectroscopy (AAS), applying $AgNO_3$ standard solution after digesting the silver containing samples in HF and $HNO_3$.

TEM images were taken by using a MORGAGNI 268D TEM (100 kV; W filament; point-resolution = 0.5 nm) electron microscope. Samples were suspended in small amount of ethanol and a drop of suspension was deposited onto copper grid covered by carbon supporting film and dried at ambient.

Thermogravimetric measurements were performed with a Setaram TG92 instrument with a heating rate of 5 K/min in nitrogen flow.

Attenuated Total Reflection Infrared (ATR-FTIR) spectra were recorded by means of a Varian Scimitar 2000 FTIR spectrometer equipped with a MCT (mercury-cadmium-tellur) detector and a single reflection ATR unit (SPECAC "Golden Gate") with diamond ATR element. In general, 128 scans and 4 $cm^{-1}$ resolution were applied. For all spectra ATR-correction was performed (Varian ResPro 4.0 software).

### 2.6. In-vitro release studies

For *in vitro* release studies, 2 mg of the propolis loaded silica particles were incubated in 200 ml phosphate buffer (pH = 5.5) at 37 °C under stirring (100 rpm). At appropriate time intervals, 5 ml samples were withdrawn and replaced by fresh buffer. The withdrawn samples were centrifuged at 15,000 rpm for 15 min and the concentration of the released drug was determined by UV-spectrophotometry at a wavelength of 292 nm (Jasco V-670). The concentration of the released poplar propolis was calculated according to the standard curves prepared in pH = 5.5 solution (r > 0.9993). The released Ag was determined by Atomic Absorption Spectroscopy.

### 2.7. In-vitro antimicrobial tests

Antibacterial and antifungal activities of the samples were evaluated using the agar well diffusion test [28] according to CLSI procedures [29]. Three human pathogens (*Staphylococcus aureus* NBIMCC 3359, *Escherichia coli* SAIM WF+ and Candida albicans SAIM 562) were used as test organisms. Briefly, 100 μl of bacterial and fungal suspensions (1.0 × 105 CFU/$ml^{-1}$) were spread on nutrient agar (CM0003, Thermo Scientific-Oxoid, UK) plates, left to dry, and then 10-mm diameter wells were made. Aliquots of 200 μL of the sample solutions containing 0.4 mg of the sample in distilled water were added to each well. The negative control wells were filled with the same volume of the solvent. Petri plates were left at 4 °C for 4 h for pre-diffusion and incubated at 37 °C in darkness overnight. Each plate was examined for symmetrical inhibition circles around the discs. Referent antimicrobial drugs with clinical use will serve as quality (positive) control for right interpretation of the results according to the recommendations of EUCAST [30]: streptomycin and nystatin. Zones of inhibition: streptomycin against *S. aureus:* 28 + 1; streptomycin against *Escherichia coli* 0, nystatin against *C. albicans* 32 + 1.

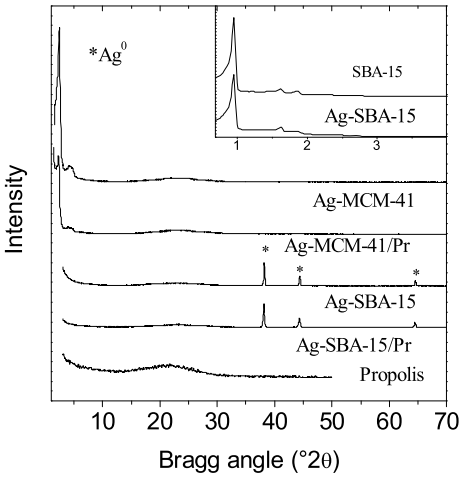



**Fig. 1.** XRD patterns of silver containing silica samples and their propolis loaded varieties.

## 3. Results and discussion

### 3.1. Characterization of silver containing nanoporous silica materials

XRD powder patterns of pure silica and silver containing SBA-15 and MCM-41 materials, and their propolis loaded varieties are shown in Fig. 1. XRD pattern of pure silica SBA-15 at low 2θ° region confirms the formation of well-ordered 2D hexagonal structure. Some intensity decrease of reflections was registered for Ag-SBA-15 sample compared to the initial SBA-15 material (Fig. 1). Ag-MCM-41 samples prepared by template ion-exchange method also show the typical patterns of highly ordered hexagonal phase with intensive (100) reflection. Reflections of metallic silver can also be observed at higher angles for both materials, but their intensity is much lower (slightly over the detection limit) on Ag-MCM-41 than on Ag-SBA-15 sample. According to AAS results (Table 2) the silver content of Ag-MCM-41 sample is only slightly lower than that of Ag-SBA-15. The alteration between the two samples can be due to their different preparation methods. By ion-exchange method in Ag-MCM-41 sample probably more ionic silver species connected to silica matrix were formed. The appearance of metallic silver on the pattern is an indication of the formation of silver crystallites bigger than ~5 nm, according to the Sherrer equation [6]. These nanoparticles can be found as a separate phase among the silica particles or attached to the outer surface of the silica support. No significant changes, only a small decrease can be observed in the unit cell and pore size of Ag-MCM-41 sample (Table 2) compared to the pure silica variety.

The $N_2$ adsorption data (Fig. 2) are in good accordance with the results from XRD. Textural parameters are summarized in Table 2. The nitrogen physisorption isotherms of pure silica and silver modified MCM-41 materials show the typical IV type physisorption isotherm with a capillary condensation step of nitrogen between 0.2 and 0.3 relative pressures. Compared to parent silica material the specific surface area and the total pore volume of Ag-MCM-41 sample are somewhat lower which is due to partial structure deterioration. The latter can be explained by effect of template ion-exchange method, i.e. the agitation of mesoporous silica at higher temperature (80 °C) in an acidic water solution, resulting in some dissolution of silica. The $N_2$ adsorption isotherms of Ag-SBA-15 sample are of the type IV with a H1 hysteresis loop, typical for SBA-15 structures. The decrease of specific surface area and pore volume of Ag-SBA-15 sample compared to the silica one is minor and probably cannot only be due to some pore blocking effect of small silver nanoparticles, but to the variation of synthesis method by applying nitric acid instead of hydrochloric acid to avoid the precipitation of silver as AgCl.

Modification by silver does not influence the morphology of MCM-

**Table 2**
Composition and textural properties of the studied samples.

| Samples | Ag cont.[a] (mmol/g) | $a_0$[b] (nm) | BET surf. area ($m^2$/g) | Total pore vol. ($cm^3$/g) | PD[c] (nm) | Propolis cont. (mg/g) | Encapsulation efficiency (%) |
|---|---|---|---|---|---|---|---|
| MCM-41 | – | 4.4 | 1175 | 0.97 | 2.7 | – | – |
| SBA-15 | – | 10.2 | 970 | 1.20 | 6.4 | – | – |
| Ag-MCM-41 | 0.52 | 4.3 | 927 | 0.76 | 2.6 | – | – |
| Ag-SBA-15 | 0.66 | 10.6 | 698 | 1.08 | 6.6 | – | – |
| Ag-MCM-41/Pr | 0.48[d] | 4.2 | 301 | 0.35 | 2.4 | 13.6 | 72 |
| Ag-SBA-15/Pr | 0.62[d] | 10.2 | 232 | 0.59 | 6.2 | 17.1 | 86 |

[a] Determined by AAS method after digestion in HF and $HNO_3$.
[b] Unit cell parameter ($a_0 = 2d_{1\,0\,0}(3)^{-1/2}$).
[c] Mean pore diameter calculated by the BJH method.
[d] Release of Ag+ in 6 h in buffer solution determined by AAS.

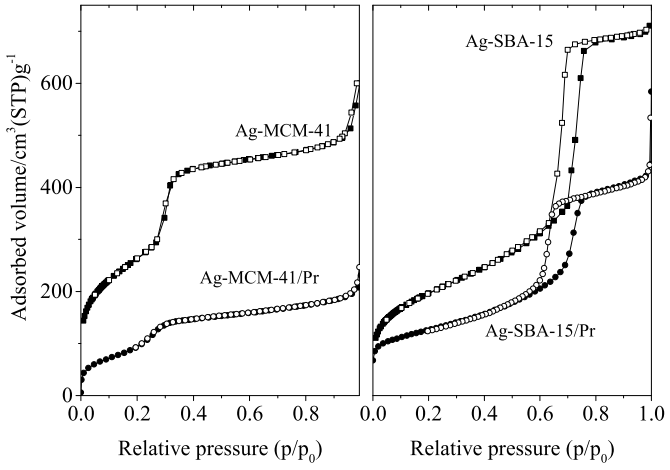



**Fig. 2.** $N_2$ physisorption isotherms of silver containing and propolis loaded varieties of nanoporous silica materials.

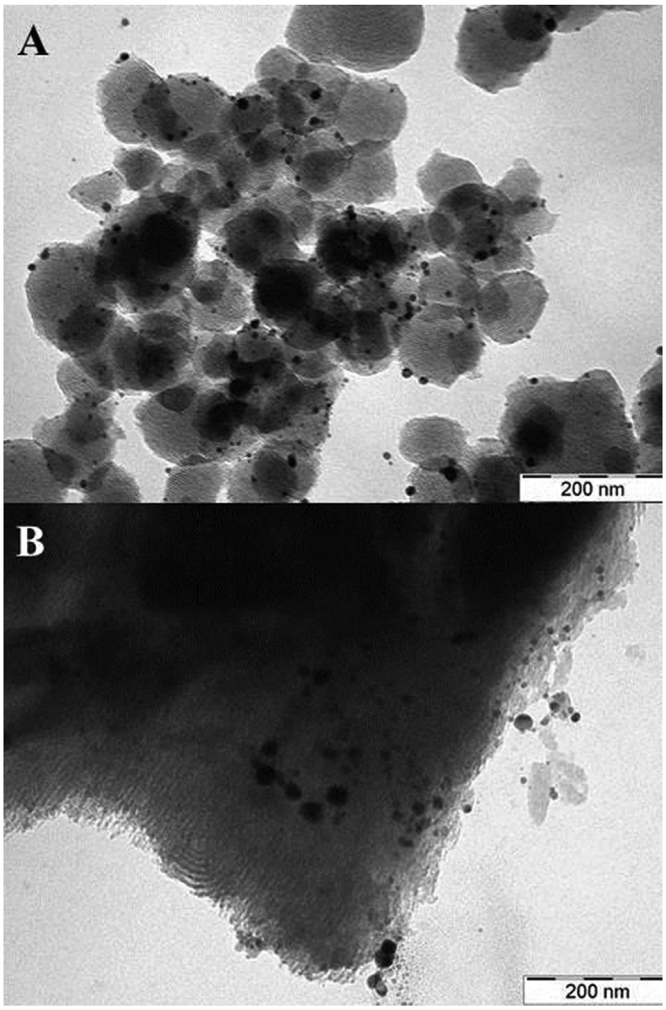



**Fig. 3.** TEM images of Ag-MCM-41(A) and Ag-SBA-15 (B) samples.

41 and SBA-15 materials as evidenced by TEM investigations (Fig. 3). Ag-MCM-41 shows the typical 100 nm spherical particles and the channel system is well preserved. Silver nanoparticles with sizes between 5 and 20 nm can be observed on the images. TEM images of Ag-SBA-15 sample exhibits also the presence of 5–20 nm sized silver nanoparticles on the external surface, and smaller 5 nm particles inside the channels can be observed as well. Formation of metallic silver nanoparticles can be explained by the reducing effect of template decomposition by calcination for both types of silica, i.e. the products of Hoffman degradation can reduce $Ag^+$ ions weakly bond to silica matrix during the synthesis procedure. The uniform, nanometer sized pores of silica carriers can hinder only to some extent the migration and agglomeration of metallic silver particles, therefore finely dispersed metallic nanoparticles formed in the channels and on the outer surface of the silica carriers.

### 3.2. Adsorption of propolis

Poplar propolis is the bee product which contains around 50 individual compounds (Table 1, [14]). Major compounds of the extract were the flavanones/dihydroflavonols (pinobanksin, pinocembrin, 3-acetylpinobanksin) and flavones/flavonols (galangin, chrysin). Propolis was adsorbed on silver containing samples using ethanol solution (70%) for 24 h. Our preliminary data showed that total encapsulation can be reached by 24 h. Encapsulation efficiency values (Table 2) with 72 and 86% for silver containing MCM-41 and SBA-15 materials supported the successful loading of propolis on the silica carriers.

XRD patterns of the propolis loaded silver silica materials do not show any reflection characteristic for propolis (Fig. 1). Dried propolis extract has an amorphous structure, and a broad peak can be observed on the pattern at 20°2θ. Compared to pure propolis the silica loaded varieties do not show the amorphous peaks, only the broad amorphous peak of silica can be observed at ~23°2θ. Similar result was found by Rocha et al. [31] by adsorbing propolis on hydroxypropyl-β-cyclodextrin support.

In contrast to XRD results, $N_2$ physisorption data really evidenced that compounds of propolis (Table 2) penetrated into the channels of silica carrier and partial pore filling was achieved (Fig. 2, Table 2). Significant decrease of BET surface area, pore volume and pore sizes are registered after the propolis loading on both MCM-41 and SBA-15 silica supports.

The amount of propolis loaded in the Ag-modified mesopores of

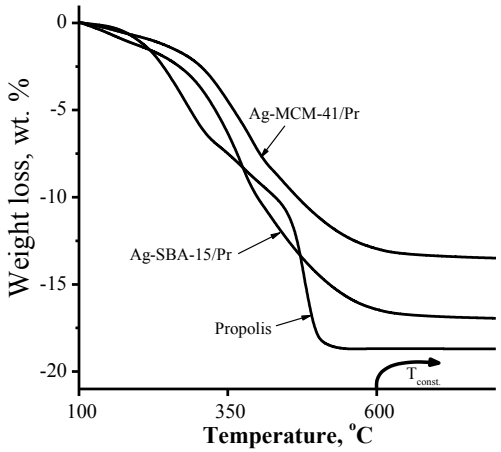



**Fig. 4.** TG curves of propolis and propolis loaded Ag-MCM-41 and Ag-SBA-15 samples.

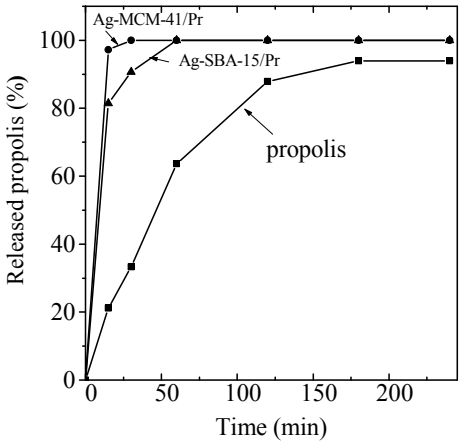



**Fig. 6.** *In vitro* release of propolis from Ag-MCM-41 and Ag-SBA-15 carriers.

MCM-41 and SBA-15 was quantified using thermogravimetry (Fig. 4). The Ag-MCM-41 sample showed lower adsorption capacity (13.6 wt.%) for propolis in comparison to its AgSBA-15 analogue (17.1 wt.%) (Fig. 4). About 46% of the pores of Ag-MCM-41 are filled with propolis if we take into account only the amount of adsorbing silica. This value is somewhat lower for Ag-SBA-15, it amounts to 34%. The lower value can be explained by more open structure of SBA-15 with wider mesopores releasing higher amount of propolis during the washing procedure following ethanolic loading (Table 2). The lower propolis adsorption capacity on Ag-MCM-41 can be explained also by the blocking of pore entrances due to the narrower pores of Ag-MCM-41 carrier. Interaction of propolis compounds with silver ions on the outer surface of MCM-41 can also contribute to this pore blocking effect.

Interaction of loaded propolis with the silica carrier was investigated by ATR FT-IR method. The ATR FT-IR spectra (Fig. 5) of propolis loaded on Ag-MCM-41 and Ag-SBA-15 show different features compared to pure propolis. The spectrum of propolis is characterized by typical $CH_2$ stretching vibrations at 2929 and 2855 $cm^{-1}$, which are clearly recognized also in the spectra of propolis loaded Ag-SBA-15 and Ag-MCM-41 samples (not shown). The most interesting part of the spectra, however, consist of bands between 1800 and 1250 $cm^{-1}$ belonging to the C=O and C=C/C-C vibrations of the flavonoid structure. In the spectrum of the pure propolis, the band at 1690 $cm^{-1}$ belongs to the stretching of C=O group, whereas bands at 1633, 1602, 1587, 1514 and 1450 $cm^{-1}$ are related to C=C and skeletal C-C stretching vibrations of flavonoid aromatic rings. The later, however, might be superposed with C-H deformations [32]. The wavenumber region below 1250 $cm^{-1}$ characteristic for primary and secondary alcohol groups of flavonoids is masked by the strong Si-O-Si vibrations of the silica matrices. After loading on Ag-MCM-41 and Ag-SBA-15, the intensity of C=O stretching of propolis is suppressed, while C=C and C=C/C-C stretching bands of flavonoid aromatic rings are shifted towards higher wavenumber. These spectral features suggest that an interactions between the silica matrices and the propolis molecules exist involving the carbonyl group and the aromatic ring of the latter.

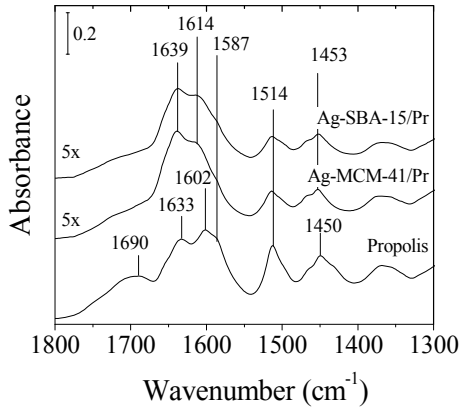



**Fig. 5.** FT-IR spectra of propolis loaded Ag-silica materials.

### 3.3. *In vitro* release of propolis

The *in vitro* release of propolis from AgMCM-41 and AgSBA-15 samples was studied in phosphate buffer at pH = 5.5. The latter pH value is widely applied for *in vitro* experiments for dermatological formulations. The drug release profiles are presented in Fig. 6. As seen in Fig. 6, non-encapsulated propolis is poorly dissolved in the selected medium, which could be expected considering its poor water solubility. In contrast, the loading of propolis on mesoporous carriers resulted in improved dissolution rate (Fig. 6). This can be explained by the higher dispersion of propolis particles confined in the channels of nanoporous silica carriers and the interaction with silver ions deposited on the support surface which is evidenced by ATR FT-IR data. The propolis release from AgMCM-41 is even faster, most probably because of the shorter diffusional route from the small particles. The simultaneous release of Ag is studied as well (Table 2). The data reveals that together with the release of propolis high release of Ag has been reached in the buffer solution, 77% for the AgMCM-41 sample and 60% for the AgSBA-15 sample. We can suggest that the released Ag together with the propolis molecules could give evidence for some synergic bioactivity.

### 3.4. *Antimicrobial efficacy of propolis loaded Ag-MCM-41 and Ag-SBA-15 samples*

Our silver and propolis containing samples were tested against the most commonly found bacteria, such as strains of ATCC *Escherichia coli 20 and Staphylococcus aureus* and fungus *Candida albicans* 562I, and were compared to pure propolis as a control (Table 3). Our results show that silver-containing nanoporous silica materials have some inherent

**Table 3**
Antimicrobial activity of propolis, Ag-modified mesoporous silicas and their propolis-loaded varieties.

| Samples | Zone of inhibition [mm] | | |
|---|---|---|---|
| | *S. aureus* 209 | *E. coli* wf + | *C. albicans* 562 I |
| Ag-SBA-15 | 5 ± 0.2 | 8 ± 0.3 | 5 ± 0.3 |
| Ag-MCM-41 | 4 ± 0.1 | 9 ± 0.5 | 5 ± 0.4 |
| Propolis | 13.7 ± 0.3 | 0 ± 0.5 | 18 ± 1 |
| Ag-SBA-15/Pr | 19 ± 0.5 | 19 ± 0.5 | 24 ± 1 |
| Ag-MCM-41/Pr | 21 ± 0.8 | 19 ± 1 | 22 ± 1 |

antibacterial and antifungal activities, but propolis shows much higher activity except for *E. coli* strain. Combining silver containing silica materials with propolis showed a synergistic effect by increasing the inhibition zone to somewhat higher value than the sum of the individual components. This is more pronounced in the case of *E. coli,* showing double increase of inhibition zone. These results indicate that propolis-loaded silver nanoporous silica samples are more effective in bacterial and fungal inhibition than pure propolis probably due to the improved solubility of the latter one. Moreover, our experiments supported the well-known fact that ionic silver relesed from silver nanoparticles has positive effect on antibacterial activity. The beneficial effect of silver is so strong that agar plates showed the original inhibition zones even after 7 days of incubation (Table 3).

## 4. Conclusions

In this study it was demonstrated for the first time that silver modified MCM-41 and SBA-15 materials are suitable carriers for propolis to design drug delivery systems with improved solubility and antimicrobial activity. It was found that mesoporous silicas can be easily modified by direct or post-synthesis methods to prepare silver nanoparticles inside the channels or on the outer surface of the particles. The mesoporous channels of the silica support is suitable for the storage of relatively high amount, 15–17 wt.% of poplar propolis. Loading of propolis from ethanolic solution on silver containing silica carriers resulted in significantly improved water solubility, probably due to its higher dispersion in the channels of the silica carrier. Antibacterial and antifungal activities investigations showed a synergistic effect of silver and propolis against widespread bacteria strains and fungus.

## Acknowledgements

Financial support by the Bulgarian-Hungarian Inter-Academic Exchange Agreement and the National Science Fund of Bulgaria (Grant DH 09/18) is greatly acknowledged.

## References

[1] S. Wang, Microporous Mesoporous Mater. 117 (2009) 1–9.
[2] M.D. Popova, Á. Szegedi, I.N. Kolev, J. Mihály, B.S. Tzankov, K.P. Yoncheva, N.G. Lambov, Inter. J. Pharm. 436 (2012) 778.
[3] M. Popova, I. Trendafilova, Á. Szegedi, J. Mihály, P. Németh, S.G. Marinova, H.A. Aleksandrov, G.N. Vayssilov, Microporous Mesoporous Mater. 228 (2016) 256–265.
[4] Z. Aziz, S.F. Abu, N.J. Chong, Burns 38 (2012) 307–318.
[5] B.S. Atiyeh, M. Costagliola, S.N. Hayek, S.A. Dibo, Burns 33 (2007) 139–148.
[6] A. Szegedi, M. Popova, K. Yoncheva, J. Makk, J. Mihalya, P. Shestakova, J. Mater. Chem. B 2 (2014) 6283–6292.
[7] L. Drago, B. Mombelli, E. De Vecchi, M.C. Fasina, L. Tocalli, M.R. Gismondo, J. Chemother. 12 (2000) 390–395.
[8] J. Sforcin, J. Ethnopharmacol. 113 (2007) 1–14.
[9] M.A.E. Watanabe, M.K. Amarante, B.J. Conti, J.M. Sforcin, J. Pharm. Pharmacol. 63 (2011) 1378–1386.
[10] R. Silva-Carvalho, F. Baltazar, C. Almeida- Aguiar, Evid. Based Complement. Altern. Med. 2015 (2015).
[11] V. Bankova, G. Boudourova-Krasteva, S. Popov, J.M. Sforcin, S.R.C. Funari, Apidologie 29 (1998) 361–367.
[12] V. Bankova, G. Boudourova-Krasteva, J.M. Sforcin, X. Frete, A. Kujumgiev, R. Maimoni-Rodella, S. Popov, Z. fur Naturforsch. 54c (1999) 401–405.
[13] A.H. Banskota, Y. Tezuka, S. Kadota, Phytother. Res. 15 (2001) 561–571.
[14] M. Popova, V. Bankova, D. Butovska, V. Petkov, B. Damyanova, A.G. Sabatini, G.L. Marcazzan, S. Bogdanov, Honeybee Sci. 24 (2) (2003) 61–66.
[15] M. Popova, S. Silici, O. Kaftanoglu, V. Bankova, Phytomedicine 12 (2005) 221–228.
[16] R. Cai, S. Wang, Y. Meng, Q. Meng, W. Zhao, X.P. Fu, J. Tohme, S.L. Wen, F. Pallottino, L. Pari, P. Menesatti, Anal. Methods 4 (2012) 2388–2395.
[17] R. Jayakumar, C. Ramya, P.S. Kumar, K.S. Snima, V.K. Lakshmanan, S.V. Nair, J. Nanopharm. Drug Deliv. 1 (2013) 150–156.
[18] S.B. de Ferreira, B.R. de A. Dias, C.S. Obregón, C.C. Gomes, R.R.A. Pereira, J.S.R. Godoy, T.I.E. Svidizinski, M.L. Bruschi, Pharm. Dev. Technol. 19 (2013) 173–180.
[19] T.G. Do Nascimento, P.F. da Silva, L.F. Azevedo, L.G. da Rocha, I.C.C. de MoraesPorto, T.F.A.L. de Moura, I.D. Basílio-Júnior, L.A.M. Grillo, C.B. Dornelas, E.J. daSilva Fonseca, E. de Jesus Oliveira, Nanoscale Res. Lett. 11 (2016) 1–16.
[20] A. Aa, O. Aa, Asian Pac. J. Trop. Biomed. J. Homepage (2011) S55–S57.
[21] X. Pascoal, D. Teresa, L. Dias, The Role of Honey and Propolis in the Treatment of Infected Wounds, Microbiology for Surgical Infections, Well Helman Press, London, 2014, pp. 221–234.
[22] H.C. Rosseto, L. de Alcântara Sica de Toledo, L.M. Belloto de Francisco, E. Esposito, Y. Lim, G. Valacchi, R. Cortesi, M.L. Bruschi, Colloids Surf. B Biointerfaces 158 (2017) 441–452.
[23] S. Huh, J. Wiench, J.-C. Yoo, M. Pruski, V.S.-Y. Lin, Chem. Mater. 15 (2003) 4247–4256.
[24] M. Iwamoto, Y. Tanaka, Catal. Surv. Jpn. 5 (2001) 25–36.
[25] W. Gac, A. Derylo-Marczewska, S. Pasieczna-Patkowska, N. Popivnyak, G. Zukocinski, J. Mol. Catal. A Chem. 268 (2007) 15–23.
[26] W. Zhu, Y. Han, L. An, Microporous Mesoporous Mater. 80 (2015) 221–226.
[27] T.H. Ong, E. Chitra, S. Ramamurthy, R.P. Siddalingam, K.H. Yuen, S.P. Ambu, F. Davamani, PLoS One 12 (3) e0174888, https://doi.org/10.1371/journal.pone.0174888.
[28] D.F. Spooner, G. Sykes, Chapter IV laboratory assessment of antibacterial activity, Methods Microbiol. 7 (1972) 211–276.
[29] P.A. Wayne (Ed.), Clinical and Laboratory Standards Institute. Performance Standards for Antimicrobial Disk and Dilution Susceptibility Tests for Bacteria Isolated from Animals, 2009, p. 28. Approved Standard M31-A33.
[30] E. Matuschek, D.F.J. Brown, G. Kahlmeter, Clin. Microbiol. Infect. 20 (2014) O255–O266.
[31] B.A. Rocha, M.R. Rodrigues, P.C.P. Bueno, A.R. de Mello Costa-Machado, M.M. de Oliveira Lima Leite Vaz, A.P. Nascimento, H.S. Barud, A.A. Berretta-Silva, J. Therm. Anal. Calorim. 108 (2012) 87–94.
[32] Y.-W. Wu, S.-Q. Sun, J. Zhao, Y. Li, Q. Zhou, J. Mol. Struct. 883–884 (2008) 48–54.